Journal of Sound and Vibration (2000) **229**(1), 199–205
Article No. jsvi.1999.2330, available online at http://www.idealibrary.com on IDEAL®

SEMI-ACTIVE FLUTTER CONTROL BY STRUCTURAL ASYMMETRY

H.-J. LIU, Z.-C. YANG AND L.-C. ZHAO

Aircraft Engineering Department, Northwestern Polytechnical University, Xi'an, People's Republic of China

(*Received* 28 *July* 1997, *and in final form* 13 *April* 1999)

1. INTRODUCTION

The mathematical model of aircraft structure for flutter analysis is usually symmetric. When different stiffness or mass properties exist between the left and right external stores, asymmetric configuration would be taken into account. Investigations [1, 2] have shown that structural asymmetry in most cases has beneficial effects for flutter prevention. This finding has led to the idea of suppressing aircraft flutter by means of disrupting the external stores symmetric state through some actuators driven by the structural-response signals. In this paper a semi-active flutter suppression scheme by using differential changes of external store stiffness is implemented and its feasibility is shown by the numerical simulation and wind tunnel tests. This scheme may provide an emergency or reserved measure to deal with the flutter encounters.

2. PARAMETRIC ANALYSIS OF EXTERNAL STORE FLUTTER

A simplified aircraft wing/body model is used to study the variation of the flutter speed with respect to the parameter of asymmetric degree between the stiffness properties of the right and left external stores. A sketch of the model is shown in Figure 1, and its relevant parameters are introduced in the last section. The symmetric configuration has equal store stiffness, represented by the store eigenfrequency ω_β. When the symmetric state is disrupted, the right and left stiffnesses change to $\omega_{\beta_1} = (1 - \delta)\omega_\beta$ and $\omega_{\beta_2} = (1 + \delta)\omega_\beta$, where δ may be called the degree of asymmetry. The curves of flutter speed, calculated by the V–g method, as functions of ω_β and for different values of δ, are shown in Figure 2. The wind tunnel test results are also depicted in Figure 2, where ● are test points for symmetric stores and □ are those for asymmetric stores ($\delta = 0{\cdot}0467$). From Figure 2 it can be seen that for the configuration with baseline store frequency $\omega_\beta = 10$ rad/s, the degree of asymmetry has the most prominent effects on flutter speed. Hence the model with the baseline store frequency $\omega_\beta = 10$ rad/s is adopted as the controlled configuration to be investigated.

0022-460X/00/010199 + 07 $35.00/0

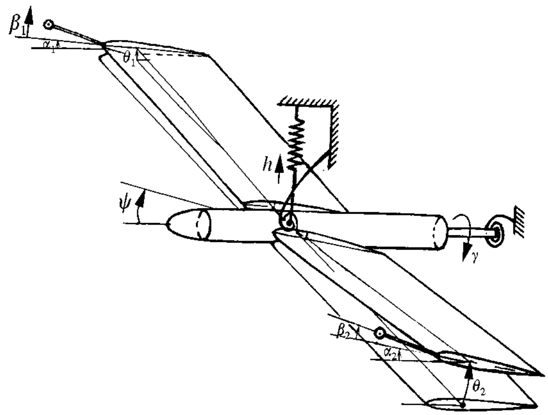

Figure 1. Sketch of the model.

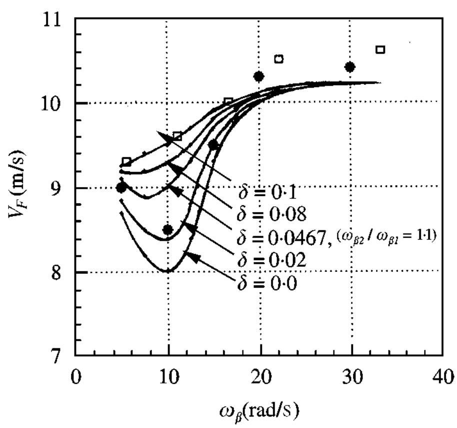

Figure 2. Flutter boundary of V_F versus ω_β.

3. AEROELASTIC EQUATION OF MOTION IN TIME DOMAIN

The equation of motion of the aeroelastic system concerned is

$$M\ddot{\xi} + K\xi = qA\xi. \tag{1}$$

For convenience of aerodynamic computation for variable store stiffness, the generalized coordinate column vector $\xi = [q_1, q_2, q_3, q_4, q_5, q_6, q_7, \beta_1, \beta_2]^{\mathrm{T}}$ is taken comprising the first seven eigenmodes of the clean wing/body (i.e., without external stores) q_1–q_7, and the left/right angle store pitching angle (i.e. β_1, β_2). In equation (1), $q = \frac{1}{2}\rho V^2$, ρ is the air density, V is the wind speed, and the stiffness matrix is

$K = diag[2{\cdot}26^2,\ 4{\cdot}14^2,\ 9{\cdot}86^2,\ 13{\cdot}16^2,\ 13{\cdot}46^2,\ 25{\cdot}96^2,\ 26{\cdot}28^2,\ \omega_{\beta_1}^2, \omega_{\beta_2}^2]$, the mass matrix is

$$M = \begin{pmatrix} 1{\cdot}01389 & 0{\cdot}00000 & -0{\cdot}00556 & -0{\cdot}00068 & -0{\cdot}01712 & 0{\cdot}02316 & -0{\cdot}07223 & 0{\cdot}00067 & 0{\cdot}00067 \\ 0{\cdot}00000 & 1{\cdot}02495 & 0{\cdot}00200 & -0{\cdot}02084 & 0{\cdot}00184 & -0{\cdot}09298 & -0{\cdot}03252 & 0{\cdot}00089 & -0{\cdot}00089 \\ -0{\cdot}00556 & 0{\cdot}00200 & 1{\cdot}00239 & -0{\cdot}00140 & 0{\cdot}00701 & -0{\cdot}01675 & 0{\cdot}02632 & -0{\cdot}00020 & -0{\cdot}00034 \\ -0{\cdot}00068 & -0{\cdot}02084 & -0{\cdot}00140 & 1{\cdot}01743 & -0{\cdot}00069 & 0{\cdot}07651 & 0{\cdot}03071 & -0{\cdot}00078 & 0{\cdot}00071 \\ -0{\cdot}01712 & 0{\cdot}00184 & 0{\cdot}00701 & -0{\cdot}00069 & 1{\cdot}02125 & -0{\cdot}03541 & 0{\cdot}08667 & -0{\cdot}00076 & -0{\cdot}00089 \\ 0{\cdot}02316 & -0{\cdot}09298 & -0{\cdot}01675 & 0{\cdot}07651 & -0{\cdot}03541 & 1{\cdot}38519 & 0{\cdot}00069 & -0{\cdot}00222 & 0{\cdot}00444 \\ -0{\cdot}07223 & -0{\cdot}03252 & 0{\cdot}02632 & 0{\cdot}03071 & 0{\cdot}08667 & 0{\cdot}00069 & 1{\cdot}41804 & -0{\cdot}00463 & -0{\cdot}00230 \\ 0{\cdot}00067 & 0{\cdot}00089 & -0{\cdot}00020 & -0{\cdot}00078 & -0{\cdot}00076 & -0{\cdot}00222 & -0{\cdot}00463 & 0{\cdot}00006 & 0{\cdot}00000 \\ 0{\cdot}00067 & -0{\cdot}00089 & -0{\cdot}00034 & 0{\cdot}00071 & -0{\cdot}00089 & 0{\cdot}00444 & -0{\cdot}00230 & 0{\cdot}00000 & 0{\cdot}00006 \end{pmatrix}.$$

By using Roger's fitting method [3], the fully unsteady aerodynamic matrix is obtained:

$$A = Q_1 + \bar{s}Q_2 + \bar{s}^2 Q_3 + \sum_{j=1}^{N} \frac{E_j \bar{s}}{\bar{s} + r_j}, \tag{2}$$

where $\bar{s} = (b/V)s$, b is a reference wing half chord length, s is the Laplace variable, $r_j (j = 1, \ldots, N)$ are N reduced frequencies in the relevant frequency region, $Q_1, Q_2, Q_3, E_j(j = 1, \ldots, N)$ are constant matrixes determined by Roger's method. Substituting equation (2) into equation (1), the equation of the motion changes to

$$M\ddot{\xi} + K\xi = q\left(Q_1 \xi + \frac{b}{V} Q_2 \dot{\xi} + \frac{b^2}{V^2} Q_3 \ddot{\xi} + \sum_{j=1}^{N} \xi_j\right), \tag{3}$$

where the aerodynamic augmented coordinates $\xi_j (j = 1, \ldots, N)$ are connected to ξ by the differential equation

$$\dot{\xi}_j = E_j \dot{\xi} - \frac{V}{b} r_j \xi_j.$$

Equation (3) should be transformed to the final computational form

$$\dot{y} = By, \tag{4}$$

where

$$B = \begin{pmatrix} 0 & I & 0 & \cdots & 0 \\ -\bar{M}^{-1}\bar{K} & -\bar{M}^{-1}\bar{C} & q\bar{M}^{-1} & \cdots & q\bar{M}^{-1} \\ 0 & E_1 & -\frac{V}{b}r_1 I & \cdots & 0 \\ \cdots & \cdots & \cdots & \cdots & \cdots \\ 0 & E_N & 0 & \cdots & -\frac{V}{b}r_N I \end{pmatrix},$$

$$\bar{M} = M - \tfrac{1}{2}\rho b^2 Q_3, \qquad \bar{C} = -\tfrac{1}{2}\rho V b Q_2,$$

$$\bar{K} = K - \tfrac{1}{2}\rho V^2 Q_1, \qquad y = \xi^{\mathrm{T}}, \dot{\xi}^{\mathrm{T}}, \xi_1^{\mathrm{T}}, \ldots, \xi_N^{\mathrm{T}})^{\mathrm{T}}$$

and I is the unit matrix.

By using the variable step fourth order Runge–Kutta method, the dynamic response is obtained from the numerical integration of equation (4).

4. SEMI-ACTIVE CONTROL STRATEGY AND NUMERICAL SIMULATION RESULTS

When feedback control is introduced to adjust the left/right store stiffness producing differential changes, the terms ω_{β_1}, $\omega_{\beta 2}$ in the stiffness matrix change in accordance. As differentially changed store stiffnesses are expressed by the formulae $\omega_{\beta_1} = (1-\delta)\omega_\beta$, $\omega_{\beta_2} = (1+\delta)\omega_\beta$, the degree of asymmetry of the left/right store stiffnesses would be adjusted by changing the single variable δ. In numerical simulation of the control process, the incremental quantity $\Delta\delta$ and the threshold value α_{th} of the response amplitude are present at first. Then at the end of a definite time interval T, comprising several integration steps to await development of the motion, the response amplitude α is read out and compared with threshold α_{th}. Judgment relating to whether δ would be increased by $\Delta\delta$ or not is to be made, depending on whether α is greater or smaller than α_{th}. The flowchart of the control program is shown in Figure 3. As mentioned above, the baseline store configuration with $\omega_\beta = 10$ rad/s is used for the present study. The flutter speed calculated by the V–g method is $V_{\mathrm{F}} = 8$ m/s. In numerical simulation, the response signal is taken from the model wing rotating motion. The threshold α_{th} is set to be $\alpha_{th} = 0{\cdot}13$, and $\Delta\delta = 0{\cdot}02$, $T = 0{\cdot}2$ s. The air speed V is 9 m/s, higher than the flutter speed of the symmetric configuration which is 8 m/s. Typical simulation results are shown in Figure 4. It can be seen that in the initial stage, i.e. the flutter occurrence stage, the response increases. As soon as the threshold value is reached, the control mechanism starts its function and the flutter response is suppressed rapidly.

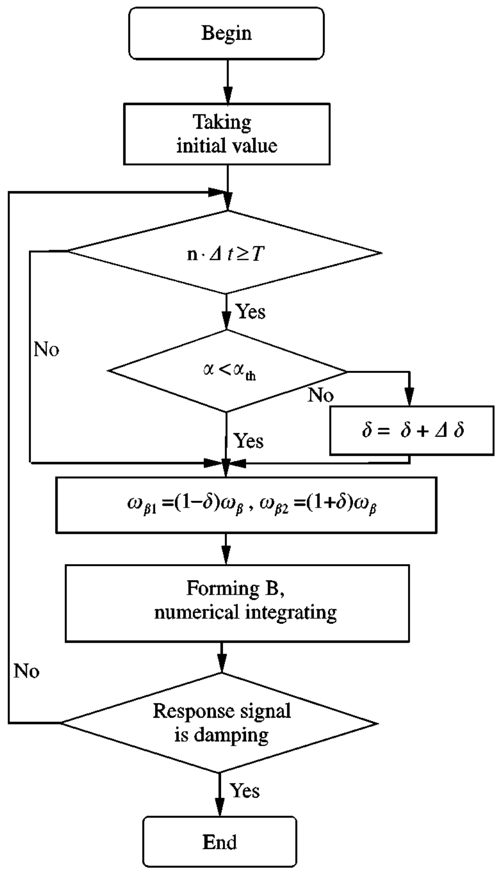

Figure 3. Flowchart of the control program.

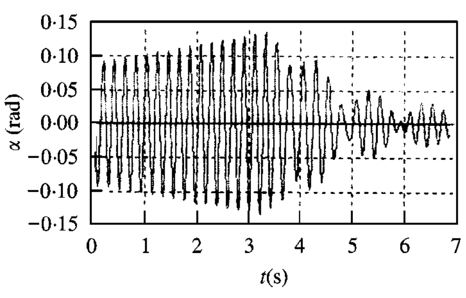

Figure 4. Numerical simulation result.

5. WIND TUNNEL TEST

The model (see Figure 1) comprises a steel frame as fuselage with separate left and right half-wings. Both half-wings are made of solid woods being regarded as absolute rigid, they are mounted to the fuselage by root springs. The half-wings can flap and rotate independent of each other. Each half-wing has a wing tip external store which can pitch relative to the wing. The whole model system has totally nine degrees of freedom, namely, fuselage heaving, pitching and rolling, left wing flapping and rotating, right wing flapping and rotating, and left/right stores pitching. All connecting and supporting springs are adjustable or replaceable to get the adequate stiffness parameters.

The automatic control function is realized by the change in the left store connection stiffness and disruption of the structural symmetry. A sketch of the control mechanism is shown in Figure 5. When flutter occurrence is detected by the computer, the minimotor W is switched on. The motor drives the guide screw to rotate with the slide block G moving along it. Thus the restoring moment produced by the spring S is changed, resulting in a change of store pitching stiffness. A dummy block having the same shape and weight as W is installed on the right store tip with the same mounting system except that the corresponding block G is not movable. The ratio of left/right store pitching frequency can be changed continuously between 1 and 1·3. Span of the half-wing = 0·3 m. The rectangular wing plan form has wing chord $c = 0{\cdot}15$ m. The wing rotation axis lies behind the wing leading edge by 0·05 m. The pivots of the stores are set just behind the wing tip leading edge. The arm length of the store is 0·08 m. Some pertinent parameters of the components of the model are: fuselage mass = 0·79 kg, fuselage pitching moment of inertia = 0·1 kg m^2, fuselage rolling moment of inertia = 0·06 kg m^2, half-wing mass = 0·38 kg, half-wing flapping moment of inertia = 0·0119 kg m^2, half-wing rotating moment of inertia = 0·001 kg m^2, store mass = 0·01 kg.

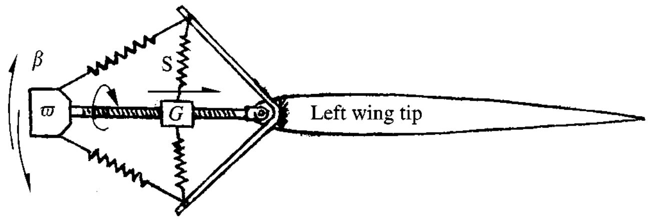

Figure 5. Sketch of the control mechanism.

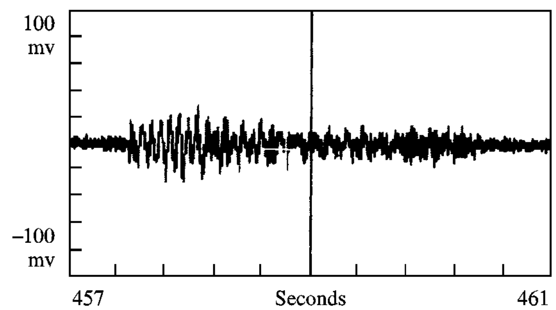

Figure 6. Wind tunnel test result.

For the left/right store pitching frequency ratio 1·1, corresponding to $\delta = 0{\cdot}0476$, the wind tunnel test results of the flutter boundary (i.e. the variation curve of flutter speed with baseline store pitching frequency) are given in Figure 2. The results are comparable to those of the calculation.

The control system comprises a data acquisition/processing unit and a driving signal/actuating unit. The whole system is controlled by a personal computer. In wind tunnel testing, the structural response signal sensed by an accelerometer is sent to the data acquisition/processing unit, and the original data is detected by the computer. When flutter is identified, an amplified driving signal is sent at once to the actuating unit. Then the motor/guide screw system mentioned above starts to work, and the structural asymmetry effect manifests itself suppressing the flutter rapidly.

The wind tunnel used was of a closed circuit type, with a circular test section of 1 m diameter and a maximum air speed of 60 m/s. In the present experiment, when the air speed was raised to 9 m/s, the response signal increased abruptly, but was only sustained for a very short time, then damped due to asymmetry control function. This process is depicted in Figure 6.

6. CONCLUDING REMARKS

For certain external store configurations, a small amount of structural asymmetry may increase the wing/store type flutter speed significantly. In this case, if feedback control is introduced to adjust automatically the stiffness of the external store on either side, then flutter can be suppressed effectively. The present study has shown feasibility of this flutter suppression scheme. In principle, the above semi-active control method has the merits of less control power required, simpler control strategy and better control effects. Certainly, more research work remains to be done for its application to practical aircraft design.

REFERENCES

1. A Lotze 1978 *AGARD Report No.* 668. Asymmetric store flutter.
2. J. K. Liu 1993 *Doctoral Dissertation. Northwestern Polytechnical University.* Investigations for the effects of structural asymmetry to aircraft dynamic characteristics and flutter. (in Chinese).
3. K. L. Roger 1997 *AGARD CP 228*. Aircraft mathematical modeling methods for active control design.